of the 100-ps time period was addressed and not just the first 5 ps, where the validity of the diffusion approximation is stretched. At very short times (<5 ps) the model presented provides only a qualitative flavor of the chemistry rather than an exact physical picture. It would be inappropriate to use a diffusion-based model to look at processes occurring on the femtosecond time scale.

4. Conclusions

This paper describes the formulation of an analytic model for the recombination kinetics that follow the photoionization of water. The model is based upon techniques developed for modeling the period of fast kinetics after the radiolysis of a liquid and involves the construction of a stochastic master equation that is solved using the independent pairs approximation. Analytic solutions are presented describing the escape probability of the hydrated electron for a variety of initial spatial distributions. Numerical solutions are shown for the time-dependent decay kinetics, and these are compared with the experimental results of Gauduel[12] and of Eisenthal.[11] To match the predictions of the analytic model to experiment, initial distributions with a root-mean-square separation between the e_{aq}^- and the OH,H_3O^+ pair of about 1.0 nm are required. This width is somewhat smaller than that obtained for the unit spur when modeling spur kinetics in radiation chemistry, 1.4 nm.[55] The difference from the result obtained here is of the expected order of magnitude, remembering the considerable discrepancy between the two different types of experiment. While the laser photoionization experiments produce prototypical unit spurs, the energy of the ejected electron is generally considerably smaller. Despite the fact that the thermalization distribution of the electron is largely determined after the electron energy is degraded to subvibrational energies, the difference in energies is obviously significant.

The purpose of the calculations described in this paper is not to give a detailed microscopic picture of the processes following photoionization but to give insight into the kinetics and the reactions that occur and so to obtain information about the spatial distribution of the reactants. The master equation approach relies upon a diffusion formalism, and it does not take into account the structural environment of the solvent in the vicinity of the reactants. No simple analytic model could possibly hope to do this. At very short times, reactions will be influenced by the solvent structure, but the calculations presented consider the kinetics over the entire 1–100-ps time period. The reactions occurring over the majority of this time frame can be adequately described by using a diffusion formalism based upon a continuum solvent.

Acknowledgment. I thank Drs. J. Chateauneuf, Y. Gauduel, and S. Pommeret for a number of interesting discussions. The work described herein was supported by the Office of Basic Energy Science of the U.S. Department of Energy. This is document NDRL-3330 of the Notre Dame Radiation Laboratory.

---

(55) Pimblott, S. M.; Pilling, M. J.; Green, N. J. B. *Radiat. Phys. Chem.* **1991**, *37*, 377.

Formation of Gas-Phase Bromine Compounds by Reaction of Solid NaBr with Gaseous $ClONO_2$, Cl_2, and BrCl at 298 K

H. N. Berko,[†] P. C. McCaslin,[‡] and B. J. Finlayson-Pitts*,[†]

Department of Chemistry and Biochemistry, California State University, Fullerton, California 92634, and UNOCAL Science and Technology Division, 376 S. Valencia, Brea, California 92621

(Received: February 4, 1991; In Final Form: April 29, 1991)

The reactions at 298 K of solid NaBr with $ClONO_2(g)$, $Cl_2(g)$, and BrCl(g) at concentrations of $(0.9–19.4) \times 10^{13}$ molecules cm^{-3} as mixtures in He flowing over the salt were investigated. The gaseous products, analyzed by mass spectrometry, were as follows: for the $ClONO_2$ reaction, Br_2 initially and subsequently BrCl and Cl_2; for the Cl_2 reaction, Br_2 followed by BrCl; and for the BrCl reaction, Br_2. Ion chromatographic analysis did not show significant replacement of bromide by chloride or nitrate in the bulk solid NaBr. Nitrate formation, however, was verified by FTIR in the $ClONO_2$–NaBr reaction. Surface analyses of the reacted NaBr salts were carried out using X-ray photoelectron spectroscopy. Detectable amounts of surface products (>50% monolayer coverage for chloride) could be seen only when NaBr was exposed to high concentrations of Cl_2 for days in a static system. Mechanisms of formation of the gaseous products in these reactions are hypothesized. The potential role of the $ClONO_2$–NaBr reaction in converting both the bromide ion in NaBr and the chlorine atom in $ClONO_2$ into highly photochemically labile gaseous compounds in the troposphere and stratosphere is discussed.

Introduction

The reactions of gases with solids at the phase interface are of great interest in a number of fields, including catalysis[1] and atmospheric chemistry.[2] Of particular interest in the latter area has been the recent observation that many reactions which are slow in the gas phase occur much more rapidly at solid interfaces. For example, the reactions of N_2O_5 and $ClONO_2$ with HCl are slow at room temperature when both are in the gas phase[3-5] but occur rapidly at temperatures of 185–200 K when the HCl is on an ice surface.[6-13] These reactions are believed to play a key role in Antarctic stratospheric chemistry by regenerating gaseous photochemically active chlorine compounds from $ClONO_2$ and HCl, which otherwise act as temporary chlorine reservoirs.

---

* To whom correspondence should be addressed.

[†] California State University.

[‡] UNOCAL Science and Technology Division.

(1) Somorjai, G. A.; Van Hove, M. A. *Prog. Surf. Sci.* **1989**, *30*, 201.

(2) Finlayson-Pitts, B. J.; Pitts, J. N., Jr. *Atmospheric Chemistry: Fundamentals and Experimental Techniques*; Wiley: New York, 1986 and references therein.

(3) Molina, L. T.; Molina, M. J.; Stachnik, R. A.; Tom, R. D. *J. Phys. Chem.* **1985**, *89*, 3779.

(4) Atkinson, R.; Aschmann, S. M.; Tuazon, E. C.; Goodman, M. A.; Winer, A. M. *J. Atmos. Chem.* **1987**, *5*, 83.

(5) Leu, M. T.; Hatakeyama, S.; Hsu, K. J. *J. Phys. Chem.* **1989**, *93*, 5778.

(6) Molina, M. J.; Tso, T. L.; Molina, L. T.; Wang, F. C. Y. *Science* **1987**, *238*, 1253.

(7) Tolbert, M. A.; Rossi, M. J.; Malhotra, R.; Golden, D. M. *Science* **1987**, *238*, 1258.

(8) Tolbert, M. A.; Rossi, M. J.; Golden, D. M. *Science* **1988**, *240*, 1018.

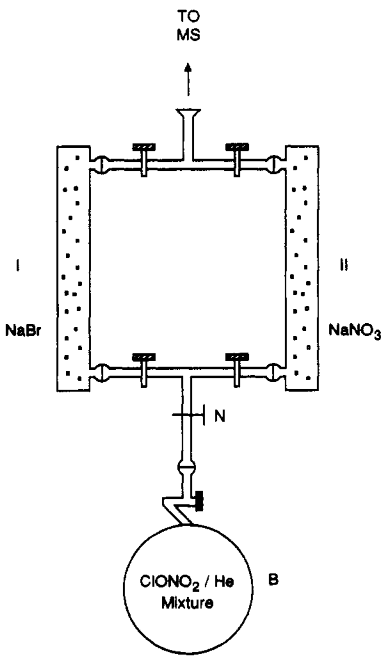

Figure 1. Diagram of flow cell apparatus. I and II are Pyrex cylindrical cells 20 cm in length and 2.5 cm in diameter; N represents the needle valve, B the 5-L gas bulb, and MS the mass spectrometer.

In the course of our studies of potential atmospheric reactions of the NaCl and NaBr components of sea-salt particles, we reported reactions 1–3:[14–17]

$$N_2O_5(g) + NaCl(s) \rightarrow ClNO_2(g) + NaNO_3(s) \quad (1)$$

$$\Delta H^{298} = -55.2 \text{ kJ mol}^{-1}$$

$$ClONO_2(g) + NaCl(s) \rightarrow Cl_2(g) + NaNO_3(s) \quad (2)$$

$$\Delta H^{298} = -82.8 \text{ kJ mol}^{-1}$$

$$N_2O_5(g) + NaBr(s) \rightarrow BrNO_2(g) + NaNO_3(s) \quad (3)$$

$$\Delta H^{298} = -46.9 \text{ kJ mol}^{-1}\,{}^{18}$$

Reactions 1 and 3 could be significant sources of halogen-containing gases in the polluted marine troposphere[14,15] and possibly in the remote Arctic.[16,17] Reactions 1 and 2 have also recently been proposed to play a role in stratospheric chemistry after some volcanic eruptions. Thus, Michelangeli et al.[19] propose that since NaCl particles were observed in the stratosphere shortly after the El Chichon eruption,[20,21] reactions 1 and 2 are at least qualitatively consistent with the stratospheric observations of decreased NO$_x$ and increased HCl in the months following the eruption.

We report here studies of the products of the reaction of ClONO$_2$ with NaBr at 298 K. The experimental observations are consistent with the initial production of BrCl, which we show also reacts with NaBr to form Br$_2$. We also report studies of the Cl$_2$–NaBr reaction. While the reaction of KBr with Cl$_2$ has been reported in the past,[22,23] the reaction conditions were much different (concentrations and reaction times both approximately 10^6 higher). This appears to be the first observation of the reactions of ClONO$_2$ and BrCl with this salt. The atmospheric implications of these reactions are discussed.

Experimental Section

Gaseous Products of the Reactions in a Flow Cell of ClONO$_2$(g), BrCl(g), and Cl$_2$(g) with NaBr(s). ClONO$_2$/He mixtures (0.07–1.5%) from a 5-L bulb initially at 1-atm pressure were reacted with NaBr by flowing the gas mixture through a needle valve to the low-pressure side of a flow system where it passed through cylindrical cells packed with NaBr (115 g) or NaNO$_3$ at 298 K (Figure 1). The effluent, at a pressure of 0.400 ± 0.010 Torr, was analyzed at various time intervals with an Extrel EMBA II quadrupole mass spectrometer, described elsewhere.[2,24] The concentrations of ClONO$_2$ over the NaBr on the low-pressure side are estimated to range from 0.9×10^{13} to 19.4×10^{13} molecules cm^{-3}. The reaction of NaBr with Cl$_2$ (2.5×10^{13} molecules cm^{-3}) and with BrCl in equilibrium with Cl$_2$/Br$_2$ (at total concentrations from 2.5×10^{13} to 14.5×10^{13} molecules cm^{-3}), all as mixtures in He, were studied in a similar manner. Fresh samples of NaBr were used for each experiment. The parallel cell packed with NaNO$_3$ was used as a control; no reactions of the gases were observed when they were passed over NaNO$_3$.

Calibration of the mass spectrometer for BrCl at m/e = 114, 116, 118 was done with BrCl from the Ethyl Corp. Chlorine calibration was done with Cl$_2$ (Union Carbide, >99.99%) using m/e = 70, 72. Bromine calibration was carried out with Br$_2$ (Fluka, >99.0%) using m/e = 160. All the halogens were degassed at 77 K and mixed with He for the calibrations.

ClONO$_2$ was prepared from the reaction of Cl$_2$O with N$_2$O$_5$ by the method of Molina et al.[25] NaBr (Fluka, >99.0%) and NaNO$_3$ (J. T. Baker, 99.6%) were sieved between 20 and 40 mesh sizes to obtain a consistent particle size range (0.4–0.9 mm) and then heated while pumping to remove adsorbed water prior to exposure to the reactant gases. Helium was from Union Carbide (Ultra High Purity, >99.999%).

Surface and Bulk Analysis of Reacted NaBr. Analyses of the surface of six samples of NaBr after reaction with ClONO$_2$, Cl$_2$, or BrCl were carried out using X-ray photoelectron spectroscopy (XPS). Each sample was prepared by sprinkling the unground crystals onto double-sided adhesive tape affixed to the sample holder. The samples were analyzed in a VG ESCALAB I instrument, using Al Kα (1486.6 eV) exciting radiation at a takeoff angle of 90° with the anode operating at 14 kV and 20 mA. The data were processed by use of an offline spectral analysis system. Peak areas were corrected by using instrumental and sensitivity factors to generate the near-surface compositional data. It should be emphasized that the XPS results give concentration values for the species near the surface. To a first approximation, the photoelectron signal decays exponentially as a function of depth below the surface. The peak positions were calculated and corrected for sample charging by charge-referencing the peaks to the ubiquitous C 1s hydrocarbon peak at 285.0 eV.

An infrared spectrum of NaBr after it had reacted with ClONO$_2$ was obtained by pressing the salt into a pellet and recording the transmission spectrum with a Mattson Cygnus 100 FTIR spectrometer. Comparison spectra were obtained for mixtures (~1%) of NaNO$_3$ and unreacted NaBr.

To investigate the possibility that these gas–solid reactions penetrated into the bulk of the solid, samples of the reacted salt were dissolved in water and analyzed by the method of indirect photometric chromatography to determine their gross anion and cation contents. A Spectra Physics SP8700 solvent delivery system

---

(9) Leu, M. T. *Geophys. Res. Lett.* **1988**, *15*, 17.

(10) Leu, M. T. *Geophys. Res. Lett.* **1988**, *15*, 851.

(11) Wolff, E. W.; Mulvaney, R.; Oates, K. *Geophys. Res. Lett.* **1989**, *16*, 487.

(12) Elliot, S.; Turco, R. P.; Toon, O. B.; Hamill, P. *Geophys. Res. Lett.* **1990**, *17*, 425.

(13) Hanson, D. R.; Mauersberger, K. *J. Phys. Chem.* **1990**, *94*, 4700.

(14) Finlayson-Pitts, B. J.; Ezell, M. J.; Pitts, J. N., Jr. *Nature* **1989**, *337*, 241.

(15) Livingston, F. E.; Finlayson-Pitts, B. J. *Geophys. Res. Lett.* **1991**, *18*, 17.

(16) Finlayson-Pitts, B. J.; Livingston, F. E.; Berko, H. N. *J. Phys. Chem.* **1989**, *93*, 4397.

(17) Finlayson-Pitts, B. J.; Livingston, F. E.; Berko, H. N. *Nature* **1990**, *343*, 622.

(18) ΔH^{f}_{298} for BrNO$_2$ is taken to be 71.1 ± 7.5 kJ mol^{-1} as reported recently by: Kreutter, K. D.; Nicovich, J. M.; Wine, P. H. *J. Phys. Chem.* **1991**, *95*, 4020.

(19) Michelangeli, D. V.; Allen, M.; Yung, Y. L. *Geophys. Res. Lett.* **1991**, *18*, 673.

(20) Woods, D. C.; Chuan, R. L. *Geophys. Res. Lett.* **1983**, *10*, 1041.

(21) Woods, D. C.; Chuan, R. L.; Rose, W. I. *Science* **1985**, *230*, 170.

(22) Morrison, J. A.; Nakayama, K. *Trans. Faraday Soc.* **1963**, *59*, 2560.

(23) Morrison, J. A.; Tuzi, Y. *Trans. Faraday Soc.* **1966**, *62*, 462.

(24) Finlayson-Pitts, B. J.; Johnson, S. N. *Atmos. Environ.* **1988**, *22*, 1107.

(25) Molina, L. T.; Spencer, J. E.; Molina, M. J. *Chem. Phys. Lett.* **1977**, *45*, 158.

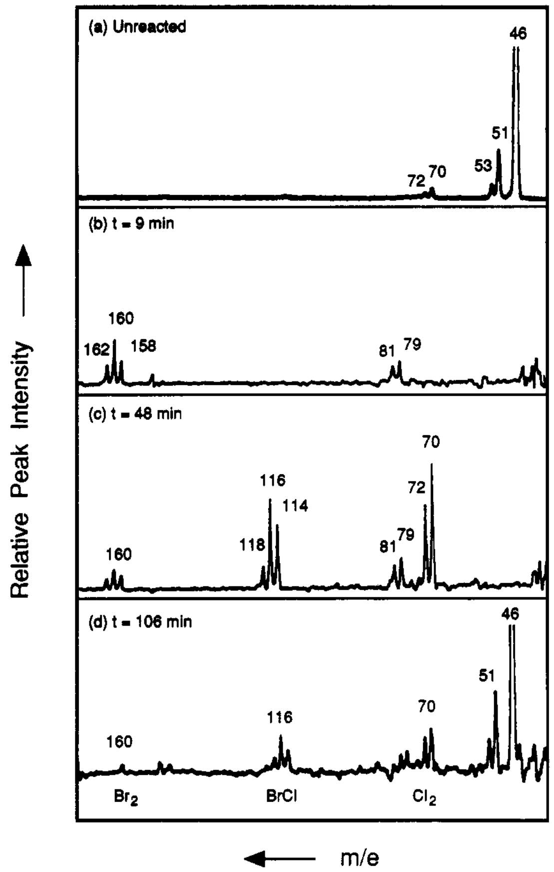

Figure 2. Mass spectra from the reaction of $ClONO_2$ with 115 g of NaBr at 298 K: (a) unreacted $ClONO_2$ (1.9×10^{14} molecules cm^{-3}), (b) after 9 min, (c) after 48 min, and (d) after 106 min.

with a Spectra Physics UV/visible, variable-wavelength, double-beam detector (Model SP8450) was used. A Vydac 302-IC405 column was used to analyze for the anions, with 2 mM phthalate buffer at pH = 5.0 as eluent; detection was at 280 nm. The cations were analyzed on a Vydac 400-IC405 column, with a $CuSO_4$ solution (5.0 mM) as eluent, and detection was at 252 nm. Solutions were injected with a Rheodyne 7125 sample injection valve fitted with a 20-μL loop. Calibration curves were obtained from standard solutions of reagent grade NaBr, NaCl, and $NaNO_3$. All salts were heated to remove absorbed water before weighing.

Reactions in a Static System of High Concentrations of $Cl_2(g)$ with NaBr(s). For comparison to experiments reported in the literature, undiluted Cl_2 (375 ± 1 Torr) was reacted with 50 g of NaBr in a 200-cm^3 glass bulb. In all cases, the reacting gas–solid mixture was kept in the dark for 11–12 days, after which the product/reactant gas mixture was diluted with He and analyzed by mass spectrometry. In addition, evidence for replacement of bromide by chloride in the bulk of the solid, as has been reported in the literature,[22,23] was sought by analyzing the ion composition of the reacted salts using ion chromatography. The surface was also analyzed by XPS as described above.

Results

Gaseous Products of the Reactions of NaBr(s) with $ClONO_2(g)$, BrCl(g), and $Cl_2(g)$ in a Flow Cell. It was anticipated, by analogy to our earlier studies of the NaCl reaction with $ClONO_2$,[14] that BrCl would be the product of the NaBr–$ClONO_2$ reaction. However, preliminary studies established that, while BrCl was observed, it was not the initial product which exited the reaction cell. As a result, extensive studies of the concentration–time profiles of the gaseous products were undertaken and the reactions of Cl_2 and BrCl, which were observed in the $ClONO_2$ reaction with NaBr, also investigated.

Figure 2 shows a typical time sequence of mass spectra obtained from the reaction of gaseous $ClONO_2$ (1.9×10^{14} molecules cm^{-3}) with solid NaBr. The spectrum of unreacted $ClONO_2$ (Figure 2a) depicts its characteristic fragmentation peaks at $m/e = 46$ due to NO_2^+ and at $m/e = 51, 53$ due to ClO^+. Peaks due to a small amount (0.4%) of impurity Cl_2 can also be seen at $m/e = 70, 72$. The same spectrum is obtained when the $ClONO_2$ is passed over $NaNO_3$ (Figure 1, cell II) as a control.

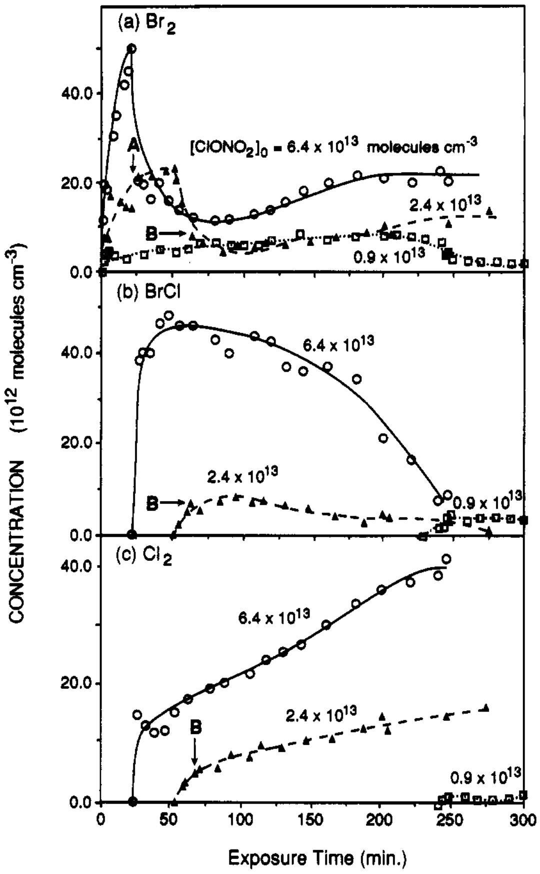

Figure 3. Concentration–time profiles for products from the reaction of 115 g of NaBr with $ClONO_2$: (a) Br_2 (b) BrCl, (c) Cl_2. Concentrations of $ClONO_2$ in He were as follows: circles, 6.4×10^{13} molecules cm^{-3}; triangles, 2.4×10^{13} molecules cm^{-3}; squares, 0.9×10^{13} molecules cm^{-3}.

The spectrum in Figure 2b shows that, after passing $ClONO_2$ over the NaBr for 9 min, only Br_2 ($m/e = 158, 160, 162$ and its fragmentation peaks at $m/e = 79, 81$) can be detected exiting the cell. Note the absence of even the large NO_2^+ peak at $m/e = 46$ and the small Cl_2 peaks at $m/e = 70, 72$, indicating both the $ClONO_2$ and the small amount of Cl_2 impurity in it have reacted completely. At 48 min (Figure 2c), BrCl ($m/e = 114, 116, 118$) and Cl_2 ($m/e = 70, 72$) along with Br_2 are present. At much longer reaction times, these product peaks decline and those due to unreacted $ClONO_2$ are again observed (Figure 2d). This sequence was typical for all the $ClONO_2$ gas mixtures reacted with NaBr.

Figure 3 shows the concentration–time profiles for the products from the reaction of NaBr with $ClONO_2$ at concentrations over the salt of $\sim 6.4 \times 10^{13}$, 2.4×10^{13}, and 0.9×10^{13} molecules cm^{-3}. The mass spectrometer was calibrated for each product, first before and then after the run. The concentrations shown in Figure 3 were obtained by a linear interpolation between the two calibrations. Because of the changing mass spectral sensitivity over the course of these rather long runs, the product concentrations shown have rather large error bars which range from ±4 to ±36%, but typically are about ±20%.

For a given initial concentration of $ClONO_2$, Br_2 peaks first; subsequently, BrCl and Cl_2 appear. The yield of BrCl is relatively constant for some time and then falls, while that of Cl_2 continues to increase with time. As seen in Figure 2d, at longer reaction times, the concentrations of all products fall and unreacted $ClONO_2$ emerges. At lower initial $ClONO_2$ concentrations (Figure 3), the sequence of production of these gaseous products remains the same but occurs at a slower rate.

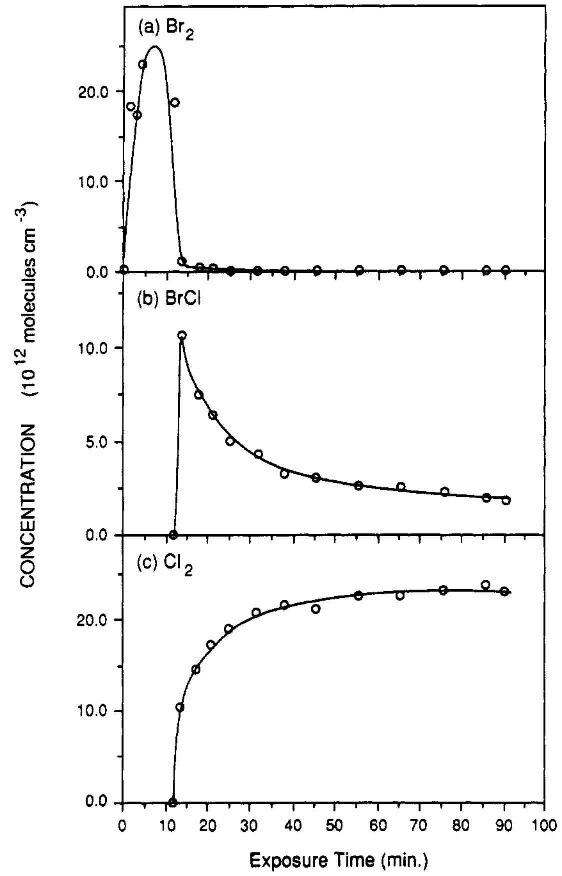

Figure 4. Concentration–time profiles for products from the reaction of Cl_2 (2.5×10^{13} molecules cm^{-3}) with 115 g of NaBr.

Since BrCl was expected to be the initial product of the NaBr–$ClONO_2$ reaction and Cl_2 was anticipated to be formed from other secondary reactions (see below), the reactions of these gases with NaBr were also studied. As seen in Figure 4, the reaction of Cl_2 (2.5×10^{13} molecules cm^{-3}) gave initially Br_2 and subsequently BrCl as the gaseous products. At longer times when production of Br_2 had ceased, a small constant concentration of BrCl along with unreacted Cl_2 (Figure 4c) emerged from the cell.

Because BrCl is in equilibrium with Br_2 and Cl_2, it is difficult to study its reaction with NaBr free of Br_2 and more importantly Cl_2, which also reacts with NaBr. In order to clarify the mechanisms, our experiments with BrCl were carried out under two conditions, one in which $[Cl_2]_0 > [Br_2]_0$ and one in which $[Br_2]_0 > [Cl_2]_0$. Figure 5 shows the sequence of production of gaseous products when a BrCl–Cl_2–Br_2 mixture in the ratio 5:6.5:1 (at a total concentration of 2.5×10^{13} molecules cm^{-3}) reacts with NaBr. Br_2 is produced first, followed by BrCl, which exits the cell at an approximately constant concentration after 23 min. Similar results were obtained for BrCl in which $[Br_2]_0 > [Cl_2]_0$.

Changes in Salt Composition after Reaction with $ClONO_2$. Table I summarizes the conditions under which NaBr was reacted with the gases in order to examine the changes occurring in the solid salt. For each of these samples, the anion-to-cation ratios $[Br^-]/[Na^+]$ and $[Cl^-]/[Na^+]$ in the bulk of the salt were determined by ion chromatography. There was no significant loss of Br^- in the bulk solid in any of the samples (i.e., all $[Br^-]/[Na^+]$ ratios were within experimental error, 95% confidence limits, of unity).

The ratios of $[Cl^-]/[Na^+]$ in the reacted samples of NaBr, although more variable, were also within experimental error of that in the unreacted salt. Thus, for unreacted NaBr, the impurity chloride was measured as $[Cl^-]/[Na^+] = (4 \pm 3) \times 10^{-4}$ (2σ), well below the manufacturers' specifications of 0.1 wt % chloride which corresponds to $[Cl^-]/[Na^+] \leq 1.6 \times 10^{-3}$. NaBr exposed to Cl_2 (sample 5, Table I) had the largest ratio: $[Cl^-]/[Na^+] = (7 \pm 3) \times 10^{-4}$, which, however, is still within experimental error of the unreacted NaBr.

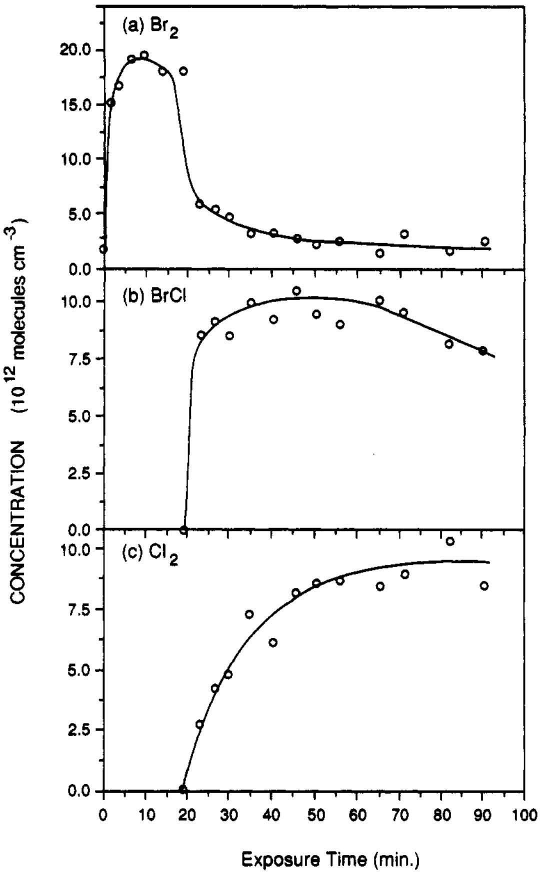

Figure 5. Concentration–time profiles for products from the reaction of a mixture of BrCl/Cl_2/Br_2 (5:6.5:1) in He (total concentration of 2.5×10^{13} molecules cm^{-3}) with 115 g of NaBr.

TABLE I: Samples of NaBr Exposed to $ClONO_2$, Cl_2, or BrCl in a Flow System and Analyzed by XPS and Ion Chromatography

sample no.	description
1	NaBr, sieved and heated but unreacted
2	NaBr exposed to $ClONO_2$ (2.4×10^{13} molecules cm^{-3}) until only Br_2 was produced (point A, Figure 3)
3	NaBr exposed to $ClONO_2$ (2.4×10^{13} molecules cm^{-3}) until BrCl and Cl_2 are also produced (point B, Figure 3)
4	NaBr exposed to $ClONO_2$ (1.9×10^{14} molecules cm^{-3}) until $ClONO_2$ emerges unreacted (Figure 2d)
5	NaBr exposed to Cl_2 (2.5×10^{13} molecules cm^{-3}) until some Cl_2 emerges unreacted
6	NaBr exposed to a mixture of BrCl/Cl_2/Br_2 in a ratio 1.0:2.6:0.1 (total concentration of 1.5×10^{14} molecules cm^{-3}) for 50 min

A search was also carried out for nitrate ion using ion chromatography. However, as seen in Figure 6, although NO_3^- can be detected in NaCl exposed to $ClONO_2$ (Figure 6b), small amounts of nitrate cannot be detected from the NaBr–$ClONO_2$ reaction (Figure 6a), at least in part because NO_3^- elutes on the tail of the Br^- peak. With our relatively low resolution for separation of the nitrate peak from the bromide peak in the NaBr samples, the upper limit we can detect for $[NO_3^-]/[Na^+]$ for all of the samples in Table I is only 2×10^{-3}.

A search for NO_3^- was therefore carried out using infrared spectroscopy on a pellet of the salt that had been exposed to $ClONO_2$ until some reactant gas was observed emerging from the cell (sample 4, Table I). As seen in Figure 7, the characteristic NO_3^- bands at 840 and 1360 cm^{-1} were observed, confirming that $NaNO_3$ is formed in the $ClONO_2$–NaBr reaction.

Reaction in a Static System of High Concentrations of $Cl_2(g)$ with NaBr(s). Earlier studies of the reactions of KBr with high (Torr) concentrations of Cl_2 for periods on the order of hours to days[22,23] showed that significant replacement of bromide by

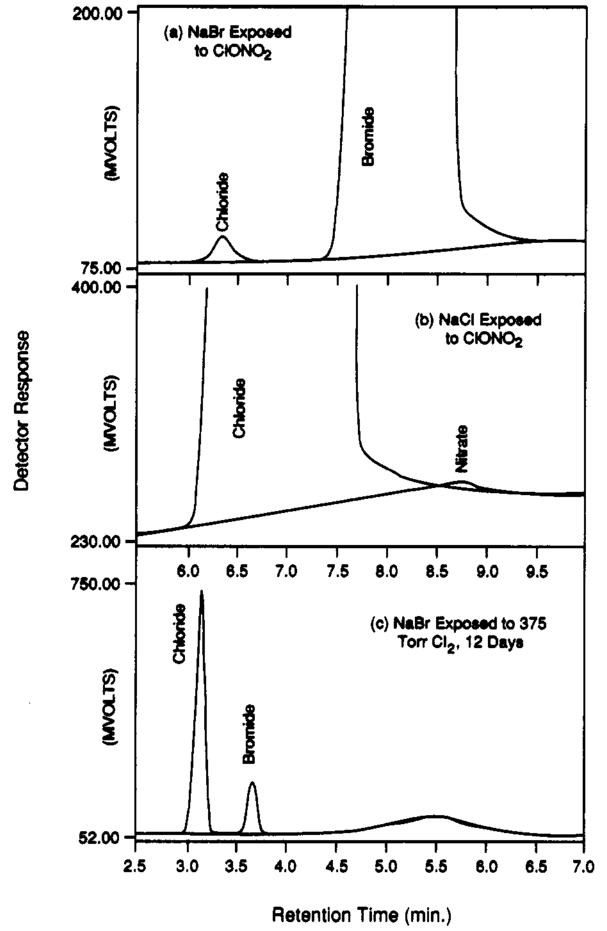

Figure 6. Ion chromatograms for anions: (a) NaBr exposed to ppm concentrations of $ClONO_2$ (sample 4, Table I), (b) NaCl exposed to 10 Torr of $ClONO_2$ for 24 h, and (c) "dark" crystals from NaBr exposed to 375 Torr of Cl_2 for 12 days (experiment 1, Table II). In (a) and (b) the analyte concentrations were 1.0 g/L and eluent flow rate was 1.0 mL/min; in (c) the analyte concentration was 0.13 g/L and the eluent flow rate was 2.0 mL/min.

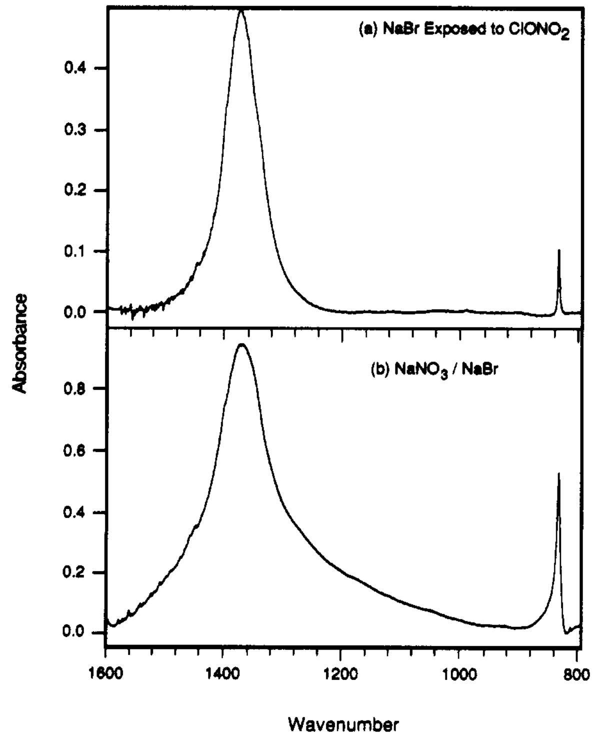

Figure 7. FTIR spectra of pellets made from (a) NaBr(s) exposed to $ClONO_2(g)$ (sample 4, Table I) and (b) $NaNO_3$/NaBr.

TABLE II: Anion/Cation Ratios from Ion Chromatography Analyses of NaBr Exposed to Cl_2 under Static Conditions[a]

		ratios ($\pm 1\sigma$)[b]	
expt	sample	$[Br^-]/[Na^+]$	$[Cl^-]/[Na^+]$
1	typical sample of reacted NaBr	0.645 (±0.007)	0.447 (±0.011)
1	dark crystals only	0.134 (±0.001)	0.723 (±0.015)
2	typical sample of reacted NaBr	0.874 (±0.013)	0.058 (±0.002)
3	unreacted NaBr	1.03 (±0.042)	$(1.3 \pm 0.1) \times 10^{-4}$

[a] Reaction conditions were 50 g of NaBr and 375 ± 1 Torr of Cl_2 in a 200-cm^3 bulb for 11–12 days in the dark. [b] Uncertainty represents analytical precision only. Overall accuracy estimated to be ±15%.

chloride (up to 100% under some conditions) occurred in the salt. For comparison to our studies under flow conditions, where much smaller gas concentrations are used and the residence time of the gases in the flow cell is of the order of minutes or less, experiments were carried out in which NaBr was exposed to 375 Torr of Cl_2 in the dark for 11–12 days. Both the salt and the gas mixture above it were then analyzed.

Mass spectrometric analyses of the residual gases from the reactions of NaBr with Cl_2 under these static conditions showed the presence of BrCl, Br_2, and unreacted Cl_2.

Table II shows the ratios of $[Br^-]/[Na^+]$ and $[Cl^-]/[Na^+]$ for typical samples of the salts from these reactions. Significant loss of bromide and gain in chloride ions in the salts were observed in both experiments 1 and 2. Most of the crystals from exposure of NaBr to Cl_2 after 11–12 days were pale yellow. However, in experiment 1, it was observed that there were a few (perhaps 1%) very dark crystals mixed in with the lighter crystals. Some of these were segregated from the exposed salt and analyzed separately. As seen from the data in Table II and the chromatogram in Figure 6c, these crystals were found to have much greater replacement of bromide by chloride than the mixture as a whole.

XPS Surface Analyses. XPS was carried out on samples 1–6 of Table I, as well as the NaBr crystals exposed to 375 Torr of Cl_2 for 12 days (experiment 1, Table II). In all cases, the surfaces were examined for the presence of C, N, O, Na, Cl, and Br. Carbon and oxygen are ubiquitous surface contaminants, while the other elements arise from the reactants. In the case of samples 1–6 from the flow experiments (Table I), the ratio of the Br 3d doublet peak area to the Na 1s peak area remained constant to within 5% on a relative basis. In addition, neither N nor Cl could be detected. The estimated detection limits for these elements in the NaBr matrix are 1% for N and 2% for Cl on an atomic basis. The Br 3d and Na 1s photoelectron peaks and the Na *KLL* Auger peaks remained constant for this series, having values indicative of the presence of NaBr.

The observed ratio R_{AB} of overlayer A (e.g., NaCl or $NaNO_3$ in this case) to substrate B (NaBr) can be related to the fractional monolayer coverage ϕ_A if it is assumed that (1) the analyzed surface is atomically flat, (2) elastic scattering of photoelectrons is minimal, and (3) the overlayer material is applied uniformly across the substrate surface (i.e., simultaneous monolayer formation and microcrystallite growth are not taken into account). The relationship between R_{AB} and ϕ_A is given by the following:[26]

$$R_{AB} = \frac{I_A/I_A^0}{I_B/I_B^0} = \frac{\phi_A\{1 - \exp[-a_A/\lambda_A(E_A) \sin\theta]\}}{(1 - \phi_A\{1 - \exp[-a_A/\lambda_A(E_B) \sin\theta]\})}$$

I_A^0 and I_B^0 are sensitivity factors, a_A is the monolayer thickness, $\lambda_A(E)$ is the inelastic mean free path of overlayer species A at energy E, and θ is the photoelectron takeoff angle with respect to the plane defined by the sample surface. The monolayer thickness a_A may be calculated from the formula

$$a_A = (A/\rho N n)^{1/3}$$

where A is the atomic weight, ρ is the density, N is Avogadro's

---

(26) Seah, M. P. *SIA, Surf. Interface Anal.* **1986**, *9*, 85.

number, and n is the number of atoms per molecule. The inelastic mean free path $\lambda_A(E)$ may be approximated by using the method of Seah and Dench[27] for inorganic molecules.

For these matrices, the above equations imply that a detection limit of 1% on an atomic basis corresponds to a fractional surface coverage *if it were a monolayer only* of approximately 0.24. A detection limit of 2% corresponds to a fractional monolayer coverage of about 0.50. Thus, nitrate must comprise less than ~24%, and chloride less than 50%, of the surface monolayer in samples 1–6 (Table I) from the exposure of NaBr to $ClONO_2$, Cl_2, or BrCl in the flow system.

The dark crystals from NaBr exposed to 375 Torr of Cl_2 in a static system (experiment 1, Table II), however, showed a large replacement of surface bromide by chloride. The atomic ratios (normalized to unity) in this sample were Br/Na = 0.24 and Cl/Na = 0.76. Thus, it appears in this sample that approximately three-fourths of the Br^- ions have been replaced by Cl^- ions within the depth analyzed by XPS. Alternatively, complete substitution of Br^- by Cl^- ions within the first three atomic layers occurred, assuming a complete substitution pattern beginning at the surface.

Discussion

The gaseous products observed in the flow system from the reaction of $ClONO_2$ with NaBr are qualitatively consistent with the following reactions:

$$ClONO_2(g) + NaBr(s) \rightarrow BrCl(g) + NaNO_3 \quad (4)$$

$$\Delta H^{298} = -118.0 \text{ kJ mol}^{-1}$$

$$BrCl(g) + NaBr(s) \rightarrow Br_2(g) + NaCl(s) \quad (5)$$

$$\Delta H^{298} = -36.8 \text{ kJ mol}^{-1}$$

$$ClONO_2(g) + NaCl(s) \rightarrow Cl_2(g) + NaNO_3(s) \quad (2)$$

$$\Delta H^{298} = -82.8 \text{ kJ mol}^{-1}$$

$$Cl_2(g) + NaBr(s) \rightarrow BrCl(g) + NaCl(s) \quad (6)$$

$$\Delta H^{298} = -40.8 \text{ kJ mol}^{-1}$$

The NaCl formed in reactions 5 and 6 is not expected to react with Br_2 or BrCl since the enthalpy changes for these reactions are both positive (+36.8 and +39.3 kJ mol^{-1}, respectively). However, NaCl is known[14] to react with $ClONO_2$, reaction 2, and hence will ultimately be converted to $NaNO_3$.

The data presented here confirm reactions 5 and 6 of BrCl and Cl_2 with NaBr. Thus, the data in Figure 4 show that Cl_2 initially produces significant concentrations of Br_2, followed by a smaller, relatively constant concentration of BrCl equivalent to conversion of approximately 8% of the incoming Cl_2 into BrCl. The initial rapid production of Br_2 is likely due to reaction 6 of surface bromide with Cl_2 to form BrCl, which as it moves through the cell over fresh NaBr surfaces is converted via reaction 5 into Br_2.

Once the surface NaBr has been completely converted to NaCl, the reaction of subsurface bromide with Cl_2 could lead to a slower generation of BrCl which would not be converted to Br_2 as it diffuses through the NaCl to the surface. On a stoichiometric basis, there is more than sufficient Cl_2 to react all of the surface NaBr, if the reaction is sufficiently fast. Thus, from the NaBr particle size and total mass in the cell, the number of NaBr molecules available on the surface is estimated to be $\sim 10^{18}$. Based on typical pressure changes in the gas bulb over these reaction times as measured in separate experiments, the number of Cl_2 molecules that have passed over the salt after the initial Br_2 peak (at 12 min) is estimated to be $\sim 10^{19}$. Such a complete reaction of the surface NaBr would be consistent with the time–concentration profiles in Figure 4. However, in this case, surface chloride should be in excess of the XPS surface analysis detection limit of approximately 50% monolayer coverage, which was not the case.

Insight into a possible alternate explanation comes from the static experiments in which NaBr was exposed to high (375 Torr) concentrations of Cl_2 for 11–12 days. Visual observation of the production of some darker crystals suggests that, even in a sample of apparently homogeneous NaBr, some crystals may have significantly higher reactivity. This was confirmed by both the XPS and ion chromatography which showed the darker crystals had undergone much more bromide replacement than the lighter crystals, indicating they were much more reactive toward Cl_2.

Since the source and pretreatment of NaBr were the same in the flow as in the static experiments, it is reasonable to expect that in the flow studies there was also a small but significant population of these more reactive crystals. The initial "burst" of Br_2 may then be due to conversion of the more reactive crystals into NaCl, while the subsequent slower production of smaller concentrations of BrCl may be due to slower reaction of the majority of the NaBr with Cl_2. If this alternate explanation is correct, it suggests that the reaction of BrCl with the majority of the NaBr crystals is slower than the Cl_2–NaBr reaction, so that it is not converted to Br_2 prior to exiting the cell.

The reaction of the $BrCl/Cl_2/Br_2$ mixture with NaBr also generates a large initial Br_2 peak (Figure 5). In a similar experiment with higher gas concentrations (Table I, sample 6), replacement of the salt surface bromide by chloride was below the XPS detection limit of 50% for monolayer coverage. This again indicates that the initial production of Br_2 cannot be attributed to complete reaction of the surface bromide but may be due to the most reactive NaBr crystals in the cell being converted to NaCl. The concentration of BrCl exiting the cell after approximately 45 min, $\sim 1.0 \times 10^{13}$ molecules cm^{-3}, is within experimental error of the initial BrCl concentration. An 8% conversion of the coreactant Cl_2 into BrCl in this experiment, similar to that seen in Figure 4, would be expected to generate a concentration of BrCl of $\sim 1 \times 10^{12}$ molecules cm^{-3}. This additional BrCl is difficult to distinguish, within the accuracy of the concentration measurements, on top of the initial BrCl concentration of $\sim 1 \times 10^{13}$ molecules cm^{-3}. However, the observation of BrCl at longer reaction times supports the earlier suggestion from the Cl_2 experiments that the reaction of BrCl with most NaBr crystals is relatively slow. This is also supported by the measured Br_2 concentration after 40 min being equal to its initial concentration; no additional Br_2 appears to be formed.

Returning to the $ClONO_2$ experiment, the first rapid production of Br_2 (Figures 2b and 3a) is thus most reasonably assigned to the most reactive NaBr crystals undergoing reactions 4 and 5. It is noteworthy that the total number of molecules of $ClONO_2$ that have passed over the NaBr at the time of this first Br_2 peak is approximately the same regardless of the initial concentration of $ClONO_2$. That is, $[ClONO_2]_0 t$, where t is the time to the initial Br_2 peak, is approximately constant to ±20%. (Although the flow rate of the gaseous reactant was not measured in these experiments, it was held approximately constant in all runs.) This is consistent with a certain fraction of the NaBr crystals being available for the initial rapid reaction to form Br_2. As in the Cl_2 flow experiments discussed above, the number of $ClONO_2$ molecules to which the salt has been exposed at the time of the Br_2 peak exceeds the available surface NaBr by approximately an order of magnitude.

After the first Br_2 peak, the reaction of the majority of the crystals with $ClONO_2$ forms BrCl; at these longer exposure times, the conversion of BrCl to Br_2 must be slower than its rate of formation, based on the results of the Cl_2 and BrCl experiments. As a result, BrCl is now observed as a product.

However, the production of both Br_2 and Cl_2 simultaneously at longer reaction times is puzzling. Thus, the results of the experiments with Cl_2 and $BrCl/Cl_2/Br_2$ mixtures (Figures 4 and 5) suggest that, after the surface of the most reactive crystals has been converted, BrCl does not react rapidly with NaBr to form Br_2 and NaCl: If reaction 2 of $ClONO_2$ with NaCl is the source of Cl_2, the increasing Cl_2 yield (Figure 3c) suggests there must be a source of NaCl, yet reaction 5 appears from the earlier experiments to be too slow to provide the NaCl at these longer reaction times.

A potential source of molecular bromine and chlorine is the thermal decomposition of the BrCl product:

---

(27) Seah, M. P.; Dench, W. A. *SIA, Surf. Interface Anal.* **1979**, *1*, 2.

$$2BrCl(g) \rightleftarrows Br_2(g) + Cl_2(g) \qquad (7)$$

$$\Delta H^{298} = -29.3 \text{ kJ mol}^{-1}$$

The kinetics[28] of this reaction, if it occurs solely in the gas phase, are too slow ($k_7 \leq 8 \times 10^{-24}$ cm^3 molecule^{-1} s^{-1}) to explain the production of the observed concentrations of Br_2 and Cl_2. This reaction has been reported to be catalyzed by surfaces.[28] However, the simultaneous production of Br_2 and Cl_2 is unlikely to be due to surface catalysis of reaction 7 by NaBr because Br_2 production was not observed simultaneously with Cl_2 when BrCl was formed in the Cl_2–NaBr reaction (Figure 4) or when BrCl was reacted with NaBr directly (Figure 5). Catalysis of the decomposition of BrCl by surface $NaNO_3$ can be ruled out by the lack of formation of additional Br_2 when the $BrCl/Cl_2/Br_2$ mixture was passed over $NaNO_3$.

The reaction of BrCl with $ClONO_2$

$$BrCl(g) + ClONO_2(g) \rightarrow Cl_2(g) + BrONO_2(g) \qquad (8)$$

is nearly thermoneutral ($\Delta H^{298} = +12.6$ kJ mol^{-1}). Such reactions are often catalyzed by surfaces, a notable example being the hydrolysis[29] of gaseous $ClONO_2$. While this could explain the formation of Cl_2, it does not explain the simultaneous formation of Br_2. In addition, BrO fragment peaks at $m/e = 95, 97$ due to $BrONO_2$ were not observed by mass spectrometry. Finally, a search for $BrONO_2$ by FTIR when BrCl (1.4×10^{15} molecules cm^{-3}) and $ClONO_2$ (5.0×10^{15} molecules cm^{-3}) were mixed in the presence and absence of $NaNO_3$ or NaBr, for 7–30 min, proved unsuccessful.

While the reactions forming Br_2 and Cl_2 at longer times in the $ClONO_2$–NaBr reaction thus remain unclear, the mass balance for the gaseous products is within experimental error of 100%. For example, as seen in Figure 3, with an initial $ClONO_2$ concentration of 2.4×10^{13} molecules cm^{-3} and at a reaction time of 96 min, BrCl peaks at 8.4×10^{12} molecules cm^{-3} and the concentrations of Cl_2 and Br_2 are 7.8×10^{12} and 5.7×10^{12} molecules cm^{-3}, respectively. From reactions 2 and 4–6, these product yields should sum to the initial $ClONO_2$ concentration. The observed products account for all of the initial $ClONO_2$ (91%), within experimental error.

It is not surprising that XPS of samples of NaBr exposed to $ClONO_2$ (Table I, samples 2–4) did not show measurable amounts of chloride, from reactions 5 and 6, on the surface. As it is formed, the NaCl will be converted to $NaNO_3$ by reaction 2 with $ClONO_2$. As discussed earlier, the detection limit on Cl^- of 2% on atomic basis corresponds to a fractional monolayer coverage of approximately 50%. Thus, if the reactions are restricted to the surface and NaCl is being reacted as it is formed, it may well be present on the surface but at monolayer coverages less than 50%.

Nitrate was not detected in any of these samples by XPS, indicating that if it is formed only at the surface, it must comprise less than approximately 25% of a monolayer. However, in NaBr exposed to $ClONO_2$ until the gaseous reactant began to emerge unreacted from the cell (sample 4, Table I) nitrate was observed by transmission FTIR (Figure 7), confirming that it is formed as expected from reactions 2 and 4. It is rather surprising that in the crystals examined by XPS, however, bromide must still represent at least 75% of the anionic surface sites.

The lack of significant changes in the bulk salt composition seen by ion chromatography indicates that the reactions in the flow cell do not penetrate into the interior of the salt significantly under these reaction conditions. With the particle size used in these experiments, the amount of NaBr on the surface compared to that in the bulk is about 1.4×10^{-4}%. If the surface bromide were completely replaced by chloride or nitrate, the concentrations of the product anions would be below the estimated detection limit of 5×10^{-4}% for chloride and 2×10^{-3}% for a completely resolved nitrate peak.

However, in our static experiments under conditions similar to that used by Morrison and co-workers,[22,23] we did observe significant replacement of bromide by chloride in agreement with their observations. The difference between the flow cell reactions and the static experiments includes much higher concentrations and longer reaction times, both increased by approximately 10^6 under the static reaction conditions. To replace bromide in the bulk, either the reactant gas or the surface chloride, once formed, must diffuse into the salt. The diffusion of Cl^- into NaBr[30] and into ice crystals[11] is slow. Thus, reactions in the bulk may be due to diffusion of the reactant gas into the salt, so it is not surprising that it does not occur during the relatively short reaction times in the flow cell.

Reaction of the halide ion at the surface with gaseous $ClONO_2$, Cl_2, and BrCl is not surprising, given the structure of the surface layer. Recent atomic force microscopic experiments[31] show that the (001) NaCl surface appears corrugated, due to the larger chloride ion projecting from the surface. Thus, the halide ions are readily available for interaction with reactive gases such as $ClONO_2$. The formation of crystals of differing color as well as differing composition both in the bulk and at the surface during the Cl_2–NaCl reaction suggests that the detailed nature of the surface may vary significantly even in this ostensibly homogeneous sample, leading to quite different reactivities toward gases such as Cl_2. It is possible that the apparent variation in crystal reactivity may be traced to the presence of exposed planes possessing arrangements of atoms more favorable for reacting with these gases.[32,33] Probing these differences and their impact on the gas–surface chemistry by using techniques such as atomic force microscopy is therefore important.

Atmospheric Implications. The atmospheric significance of these reactions will clearly depend on the gas–solid reaction efficiency and how it is affected by temperature, relative humidity, etc. Studies to measure the kinetics of these heterogeneous reactions are currently under way in this laboratory. However, if they are sufficiently fast, they may be important in the troposphere and, under some conditions, possibly in the stratosphere as well.

Troposphere. Small (ppt) concentrations of $ClONO_2$ have been predicted[34] in the marine troposphere from the ClO reaction with NO_2. Under these conditions, the chlorine in $ClONO_2$ could be recycled by reaction with NaBr in sea salt particles, forming BrCl. This reaction would simultaneously convert bromide from the salt and chlorine from $ClONO_2$ into a photochemically active form.

Stratosphere. $ClONO_2$, formed in the stratosphere from the reaction of ClO with NO_2, acts as a temporary sink for active chlorine, thus slowing the ozone destruction process. Reactions that convert chlorine nitrate into chlorine atoms or into photochemically labile compounds that photolyze rapidly to atomic chlorine, such as its reaction with HCl in ice, are thus of great importance.

Chloride salt particles were observed in the stratosphere about a month after the eruption of El Chichon in late March and early April 1982[20,21] as well as after other volcanic eruptions.[35] In the El Chichon case, Woods et al.[21] suggested that the NaCl is converted into HCl by reaction with sulfuric acid. On the basis of the experimental work of Finlayson-Pitts and co-workers,[14,15] Michelangeli et al.[19] have proposed that the reaction of NaCl with N_2O_5 and/or $ClONO_2$ may be responsible for conversion first into photochemically active species such as $ClNO_2$ and Cl_2 and subsequently into HCl.

It is not clear whether small amounts of bromide accompany the chloride production from such volcanic activity. If NaBr is also present with NaCl, the reaction of $ClONO_2$ described here could serve as another mechanism for recycling chlorine into a photochemically active form, while simultaneously producing

---

[28] Wen, W. Y.; Noyes, R. M. *Int. J. Chem. Kinet.* **1974**, *6*, 29.

[29] Rowland, F. S.; Sato, H.; Khwaja, H.; Elliott, S. M. *J. Phys. Chem.* **1986**, *90*, 1985.

[30] Harrison, L. G.; Koga, Y. *Proc. R. Soc. London, A* **1972**, *327*, 97.

[31] Meyer, G.; Amer, N. M. *Appl. Phys. Lett.* **1990**, *56*, 2100.

[32] Somorjai, G. A.; Van Hove, M. A. *Catal. Lett.* **1988**, *1*, 433.

[33] Jones, R. G. *Prog. Surf. Sci.* **1988**, *27*, 25.

[34] Singh, H. B.; Kasting, J. F. *J. Atmos. Chem.* **1988**, *7*, 261.

[35] Rose, W. I., Jr.; Chuan, R. L.; Cadle, R. D.; Woods, D. C. *Am. J. Sci.* **1980**, *280*, 671.

reactive bromine which also participates in O_3 destruction.[36]

Conclusions

Solid NaBr reacts with gaseous $ClONO_2$ to form BrCl and with BrCl to form Br_2. In agreement with earlier work in the literature,[22,23] NaBr produces BrCl on reaction with Cl_2. The data suggest that a small fraction of the crystals from an ostensibly homogeneous sample of NaBr are much more reactive than the majority of the crystals.

The reaction of NaBr with $ClONO_2$ is a potential mechanism for generating bromine and chlorine atoms in the atmosphere via the production of photochemically labile BrCl. This reaction could occur in the troposphere with NaBr from sea salt particles and possibly in the stratosphere after the eruption of alkalic volcanoes such as El Chichon. A search for bromide particles injected into the stratosphere after the eruption of such volcanoes in the future is therefore important.

Acknowledgment. We are grateful to the National Science Foundation (Grants ATM-9005321 and ATM-8704229), and especially Dr.'s Richard Carrigan and Jarvis Moyers, for support of this work. We also thank Dr. J. N. Pitts Jr. for helpful discussions and comments on the manuscript, Dr. Yuk L. Yung for making a preprint of his work available before publication, Dr. R. J. Lukasiewicz for facilitating the experiments, and the Ethyl Corp. for supplying the BrCl.

---

(36) Yung, Y. L.; Pinto, J. P.; Watson, R. T.; Sander, S. P. *J. Atmos. Sci.* **1980**, *37*, 339.

Discovery of N_2 Formation after Selective Pumping of the 0^0 State of Difluorodiazirine, F_2CN_2

Hans Sieber,[†] William R. Moomaw,[‡] Hans Jürgen Neusser,* and Edward W. Schlag

Institut für Physikalische und Theoretische Chemie der Technischen Universität München,
Lichtenbergstrasse 4, W-8046 Garching, Germany

(Received: February 7, 1991;
In Final Form: March 28, 1991)

The vibrationless 0^0 state of the $S_1(\tilde{A}^1B_1) \leftarrow S_0(\tilde{X}^1A_1)$ transition in difluorodiazirine was excited with UV light by using a narrow-bandwidth (0.3 cm^{-1}) pulsed dye laser. For the first time it was shown that dissociation occurs at this low energy and molecular nitrogen is a dissociation product. After photolysis, N_2 was detected by 2+2 multiphoton ionization via the resonantly enhanced rotationally resolved $\tilde{A}^1\Pi_g$ ($v' = 3$) $\leftarrow$ $\tilde{X}^1\Sigma_g^+$ ($v'' = 0$) transition. The dissociation quantum yield is only 2% after excitation of the electronic origin of the S_1 state. From this result and our previous Doppler-free two-photon measurements of the same 0^0_0 band, we conclude that the dissociation proceeds via a coupling of the $\tilde{A}^1B_1$ state to the $\tilde{X}^1A_1$ electronic ground state.

Introduction

Diazirines are unique molecules because of their three-membered CNN ring. A typical representative of this class of compounds is the five-atom molecule difluorodiazirine, F_2CN_2. It is known that the ring of this molecule can easily decompose into the difluorocarbene diradical, $[F_2C:]$, and nitrogen, N_2, after absorption of ultraviolet radiation:[1]

$$F_2CN_2 \xrightarrow{h\nu} [F_2C:] + N_2 \rightarrow F_2C{=}CF_2 + N_2$$

This unimolecular dissociation is assumed to be the same primary step for thermal decomposition, but thermolysis leads to a complex mixture of fluorinated products,[1-3] probably due to secondary reactions.

The lifetime of room-temperature difluorocarbene, $[F_2C:]$, after UV excitation of 5.5 Torr of F_2CN_2 seeded in 500 Torr of N_2 in the above reaction has been measured to be about 2.5 ms.[4] In matrices at very low temperature ($\approx$4 K) the difluorocarbene is stable for longer periods of time. For this reason, the photolysis of difluorodiazirine in N_2 and Ar matrices has been used to produce the difluorocarbene radical.[4-8] The light source for the photolysis has been either a medium-pressure mercury lamp or a flash lamp.

In these experiments no sharp excitation wavelength was used for the photolysis. Therefore, neither the dissociation limit nor the dependence of the dissociation efficiency on the photon energy could be determined. From the flash photolysis experiments it was concluded that the dissociation quantum yield is nearly 100% for an excitation wavelength ranging from 200 to 500 nm.[4,6] Milligan et al.[5] reported dissociation of difluorodiazirine at wavelengths longer than 300 nm. This corresponds to an excess energy of more than 5000 cm^{-1} above the origin of the allowed $S_1(\tilde{A}^1B_1) \leftarrow S_0(\tilde{X}^1A_1)$, $n\pi^*$ transition, which is located at 352 nm.[9-13] In an experiment with vibrational selective excitation Vandersall and Rice[11] found that the dissociation rate increases with increasing excess energy. This was concluded from the measured decrease of the fluorescence quantum efficiency at increasing energies, i.e., the 1^1 vibrational level with an excess energy of about 1450 cm^{-1} (around 335 nm) or vibrational levels with even higher excess energy. The authors presented no information on the dissociation limit and the dissociation quantum

---

[†] Present address: TÜV Bayern e.V., Westendstrasse 199, D-8000 München 21, Germany.

[‡] Tufts University, 474 Boston Avenue, Curits Hall, Medford, MA 02155.

(1) Mitsch, R. A. *J. Heterocycl. Chem.* **1964**, *1*, 59.
(2) Neuvar, E. W.; Mitsch, R. A. *J. Phys. Chem.* **1967**, *71*, 1229.
(3) Mitsch, R. A.; Neuvar, E. W.; Ogden, P. H. *J. Heterocycl. Chem.* **1967**, *4*, 389.
(4) Herr, K. C.; Pimentel, G. C. *Appl. Opt.* **1965**, *4*, 25.
(5) Milligan, D. E.; Mann, D. E.; Jacox, M. E.; Mitsch, R. A. *J. Chem. Phys.* **1964**, *41*, 1199.
(6) Schoen, L. J.; Mann, D. E. *J. Chem. Phys.* **1964**, *41*, 1514.
(7) Smith, C. E.; Jacox, M. E.; Milligan, D. E. *J. Mol. Spectrosc.* **1976**, *60*, 381.
(8) Jacox, M. E. *J. Mol. Spectrosc.* **1980**, *81*, 349.
(9) Lombardi, J. R.; Klemperer, W.; Robin, M. B.; Basch, H.; Kuebler, N. A. *J. Chem. Phys.* **1969**, *51*, 33.
(10) Hepburn, P. H.; Hollas, J. M. *J. Mol. Spectrosc.* **1974**, *50*, 126.
(11) Vandersall, M.; Rice, S. A. *J. Chem. Phys.* **1983**, *79*, 4845.
(12) Sieber, H.; Bruno, A. E.; Neusser, H. J. *J. Phys. Chem.* **1990**, *94*, 203.
(13) Sieber, H.; Riedle, E.; Neusser, H. J. *Chem. Phys. Lett.* **1990**, *169*, 191.

0022-3654/91/2095-6958$02.50/0